ELSEVIER

Journal of Organometallic Chemistry 553 (1998) 285–306

Journal of Organometallic Chemistry

Enantioselective catalysis Part 114. [1] Chirostructural analysis of bis(diphenylphosphanyl)ethane transition metal chelates [2]

Henri Brunner *, Andreas Winter, Josef Breu

Institut für Anorganische Chemie, Universität Regensburg, D-93040 Regensburg, Germany

Received 7 July 1997

Abstract

Transition metal complexes of bis(diphenylphosphanyl)ethane type ligands play an important role in asymmetric catalysis. The four phenyl substituents form a chiral array responsible for the high optical yields achieved with these ligands. In this paper we present an analysis of the phenyl ring orientations based on a search in the Cambridge Structural Database (CSD). The phenyl arrangements are not only subdivided into the well known face and edge exposed types, but they are additionally distinguished by the sign of the torsion angle M–P–C_{ipso}–C_{ortho} according to their chirality into face-P, face-M, edge-P, and edge-M. This approach allows a more differentiated examination. We found, that the phenyl rings prefer certain orientations within a small range depending on their axial or equatorial position and the ligand chirality. A comparison of these results with those of an analysis of achiral bis(diphenylphosphanyl)ethane complexes shows, that the substituents at the ligand backbone of the chiral phosphines reinforce the typical phenyl ring orientation in optically active phosphine complexes. © 1998 Elsevier Science S.A.

Keywords: Bis(diphenylphosphanyl)ethane type ligands; Phenyl ring orientation; Chirality transfer; Conformational analysis; Structural analyses

1. Introduction

Transition metal complexes of optically active bis(diphenylphosphanyl)ethane type ligands are well known to catalyse a vast variety of asymmetric reactions [2]. In the enantioselective hydrogenation of dehydroamino acids [3] but also in other reactions, e.g., the enantioselective homo Diels–Alder reaction [4,5] high optical inductions can be achieved. Therefore, it is of interest to understand the chirality transfer in the corresponding catalysts. It is known, that the four phenyl substituents of bis(diphenylposphanyl)ethane ligands, which surround the metal atom, affect the bonding of the substrate to the catalyst. X-ray structure analyses show, that bis(diphenylphosphanyl)ethane complexes are characterized by a specific puckering of the chelate ring, forcing the phenyl substituents into orientations described as axial–equatorial and face–edge exposed (Fig. 1a) [6,7]. The chirality of the chelate ring, δ in both examples of Fig. 1, is governed by the substituents of the asymmetric carbon atoms in the ethane backbone of the ligand. The small hydrogen atoms tend to orient axially (more intramolecular steric hindrance), whereas the larger substituents tend to orient equatorially (less intramolecular steric hindrance; dashed lines in Fig. 1a and b). In principle, the geometrical situation is similar to the puckered five-membered M–N–C–C–N rings of complexes of the well-known 1,2-diaminoethane type ligands (Fig. 1b) [8].

In this article, we want to show that the chiral puckering of five-membered chelate rings does not only differentiate the phenyl rings into axial–equatorial and face–edge exposed, but imposes a predominant chiral orientation on each phenyl ring. With this analysis we try to find an explanation for the transfer of the chiral

* Corresponding author.

[1] For Part 113, see Ref. [1].

[2] Dedicated to Prof. Dr. A. Müller on the occasion of his 60th birthday.

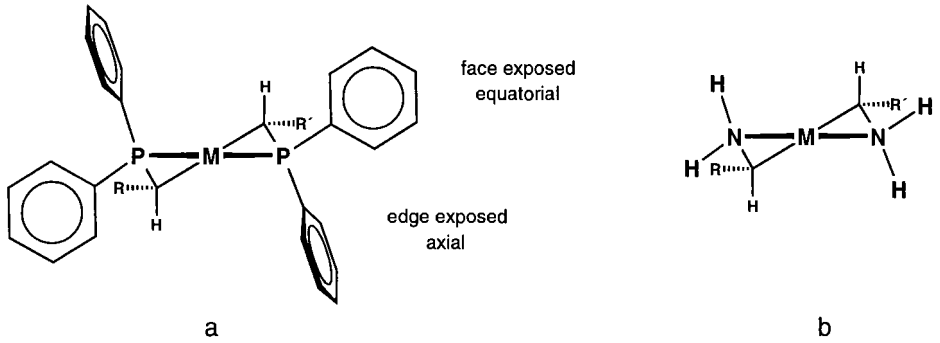

Fig. 1. Five-membered chelate rings of δ conformation (a) bis(diphenylphosphanyl)ethane complex and (b) 1,2-diaminoethane complex. The phenyl substituents in (a) show the typical axial–equatorial arrangement and face–edge exposure.

information from the ligand backbone to the metal atom, where the enantioselective reactions take place.

2. Conformational types I, II, and III and phenyl orientations edge-P, edge-M and face-P, face-M

The conformation (δ or λ) of a five-membered chelate ring is classified as previously published [9]. The P–P connecting line and the C–C bond of the ethane backbone are taken as a pair of skew lines, which determine a helix. Viewed away from the observer the two skew lines of the chelate ring in Fig. 1a define axis and tangent of a helix turning clockwise and therefore get the conformation symbol δ. The helix defined by the inverted structure would turn anti-clockwise (λ-conformation). As mentioned in the introduction, the chirality of the chelate ring is controlled by the tendency of the larger substituent of the asymmetric center to orient equatorially. Thus, λ-chirality is expected for ligands with asymmetric centers of (R)-configuration and δ-chirality for (S)-configurated ligands.

In addition to the chirality δ and λ, the conformation of five-membered chelate rings is characterized by the torsion angle P–M–P–C_{chel} within the chelate ring, called α (Fig. 2). The two torsion angles P–M–P–C_{ipso} β_{ax} and β_{eq} (Fig. 2) distinguish the two phenyl rings bonded to a P atom as to their axial or equatorial position. This differentiation is caused by the puckering of the chelate ring M–P–C–C–P. β is restricted to the interval $-\pi < \beta \leq \pi$ with β being positive if, viewing the atoms along the M–P bond with M nearer to the observer, the angle from the projection of P–M to the projection of P–C_{ipso} is traced in the clockwise sense. The lower value of β corresponds to axial position, the higher value to equatorial position.

There are two torsion angles α in each M–P–C–C–P ring. If both of them have either positive or negative values, similar in magnitude, the conformation is close to ideally puckered (type I, Fig. 3a). Normally, in such a half-chair conformation the two phenyl substituents at the phosphorus atom are clearly differentiated into axial and equatorial (Fig. 2), due to the interdependence of the α angles (torsion angles within the chelate ring) and the β angles (axial–equatorial character of the phenyl substituents).

If one angle is close to zero and the other is much larger, the conformation approaches an envelope (type II, Fig. 3b). There are also cases of a distorted envelope conformation, in which both torsion angles have different signs, one angle being small, the other large (type III, Fig. 3c). The most obvious consequence of a type III conformation is the inversion of the axial–equatorial positions of the phenyl rings on the 'flat' side (small α angle) compared to type I and type II conformations. An overall analysis shows that the 40 compounds of Table 1 retrieved from the Cambridge Structural Database (CSD) in November 1996, containing a total of 50 five-membered chelate rings M–P–C–C–P derived from chiral PP ligands, subdivide into type I (half-chair), type II (envelope) and type III (distorted envelope) conformations. The borderline between type I and type II conformations is defined as the α angle of the 'flat' side of the chelate ring being less than half of the α angle of the 'steep' side. Type II and type III conformations are separated from each other by $\alpha = 0$.

To describe the phenyl orientation in the diphenylphosphanyl groups of chelating diphosphines with respect to rotation about the P–C_{ipso} bond, the torsion angles M–P–C_{ipso}–C_{ortho} γ' and γ'' are used.

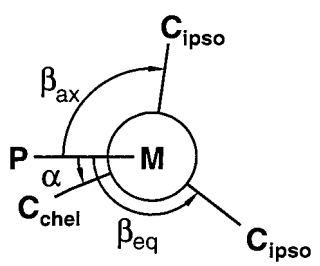

Fig. 2. Newman projection along the M–P bond. Definition of axial and equatorial phenyl positions on the basis of angles β_{ax} and β_{eq}. Angle α is a gauge for the conformation of the chelate ring.

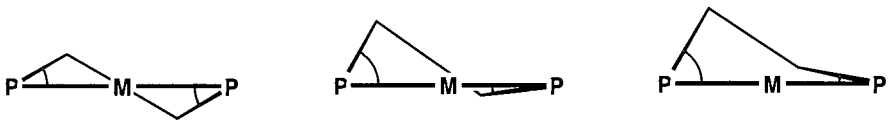

Fig. 3. Conformations of five-membered chelate rings (a) half chair conformation (type I), (b) approaching envelope conformation (type II), (c) distorted envelope conformation (type III). In each case the two angles α are indicated by an arc of a circle.

In Fig. 4, the Newman projection along the P–C_{ipso} bond of one of the $P(C_6H_5)_2$ phenyl rings is shown with the M–P bond directed horizontally. There are two such torsional angles γ' and γ'' to the two ortho C atoms. Universally, the smaller angle γ' ($|\gamma'| \leq 90°$) is used. The individual angles γ' are corrected for the nonplanarity of the phenyl substituents with the formula $\gamma = [(\gamma'/|\gamma'|)(180° - |\gamma''|) + \gamma']/2$ [46]. The averaged torsion angle is called γ, its value being close to that of γ'.

A chirality is assigned to the phenyl ring orientations as shown in Fig. 4. The bonds M–P and C_{ipso}–C_{ortho} form a pair of skew lines, which can be considered the axis and the tangent of a helix [9]. A positive torsion angle γ defines M (minus) chirality (as in Fig. 4), a negative γ P (plus) chirality.

Table 1
CSD reference codes and formulas of all the analyzed chiral compounds

Ref. code	Chirality	Formula	Ref.
BUHRIF10	*R*	(η^5-C_5H_5)Ru(prophos)Cl	[11]
BUHROL	*R*	(η^5-C_5H_5)Ru(prophos)$SnCl_3 \cdot CH_2Cl_2$	[12]
COCONO	*R*	Co(prophos)(CO)NO	[13]
FAXZIN	*R*	[(η^5-C_5H_5)Ru(prophos)C(CH_2Ph)OMe][PF_6]	[14]
FAXZOT	*R*	[(η^5-C_5H_5)Ru(prophos)(C=CHMe)][PF_6]	[14]
FUTWUM	*S*	(η^6-C_6H_5PMePh)Mo(prophos)$PMePh_2 \cdot C_6H_6$	[15]
FUTXAT	*R* + *S*	(η^6-C_6H_5PMePh)Mo(prophos)$PMePh_2 \cdot C_6H_6$	[15]
GARZEE	*R*	(η^5-C_5H_5)Ru(prophos)$S_2CH \cdot CS_2$	[16]
LAWZEO	*R*	[(η^5-indenyl)Rh(prophos)Me][BPh_4]	[17]
LIFLER	*R*	$Mn(CO)_3$(prophos)ferrocenylethynyl	[18]
CUYYAW	*S,S*	[{η^3-C_3H_2Ph(*p*-xylyl)$_2$}Pd(chiraphos)][BPh_4] · EtAc	[19]
DOCPIU	*S,S*	{(chiraphos)RuCl}$_2$(μ^2-Cl)$_3$ · 2 CH_2Cl_2	[20]
DUBTUP	*S,S*	[Rh(chiraphos)$_2$]Cl	[21]
OCPBRH	*S,S*	[(cod)Rh(chiraphos)][ClO_4] · THF	[22]
PODDAN	*S,S*	[(*t*-butyl)CH-C]$Ru_3(CO)_9$Pt(chiraphos)	[23]
SAHNEU	*S,S*	[IrH_2(chiraphos)$_2$][BF_4]	[24]
SAZTAO	*S,S*	(η^5-indenyl)Ru(chiraphos)Cl	[25]
SAZTES	*S,S*	(η^5-C_5H_5)Ru(chiraphos)Cl · CH_2Cl_2	[25]
BAVSAS	*S,S*	[(nbd)Rh(norphos)][ClO_4] · THF	[26]
CICPEJ	*R,R*	[CpFe(norphos)CO][PF_6] · C_6H_6	[27]
HATJOB	*R,R*	[(cod)Ir(norphos)][PF_6] · Et_2O	[28]
VIMBEY	*R,R*	(η^5-C_5H_5)Ru(norphos)I	[29]
CEJJEG	*R,R*	[(cod)Rh(renorphos)][ClO_4] · THF	[30]
CUNKUR	*S,S*	Ni(renorphos)Cl_2	[31]
DIRE	*R,R* + *S,S*	Ni(renorphos)$_2$	[31]
BUTWES	*R,R*	Ni[cyclo-C_5H_8(PPh_2)$_2$]$Br_2 \cdot CH_2Cl_2$	[32]
CASDOP	*S,S*	Pd{(Ph_2PCHCO)O[COC(C_5H_5)PPh_2]}I_2 · 0.5 $ClCH_2CH_2Cl$	[33]
FECDIA	*R,R*	Ni{cyclo-C_4H_6(PPh_2)$_2$}Cl_2	[34]
HAJKUJ	*S,S* + *R,R*	[Rh{cyclo-C_5H_8(PPh_2)$_2$}$_2$][BF_4] · CH_2Cl_2	[35]
SACHIN	*R,R*	[(cod)Rh{cyclo-Ph_2PCHCH_2N(CH_2Ph)CH_2CHPPh_2}][BF_4]	[36]
SOSPEV	*S,S* + *R,R*	$Re_2(O_2CPh)_2Cl_6 \cdot ReCl_2$\{cyclo-$C_5H_8$($PPh_2$)$_2$\} · $CHCl_3$	[37]
DEXFIV	*R*	[Cu◁Ph_2PCH{CH(CH_3)NH(BOC)}CH_2PPh_2▷$_2$][$CuCl_2$]	[38]
FP14	*R*	Co{Ph_2PCH($CH_2CH_2PPh_2$)CH_2PPh_2}(CO)NO	[39]
FUTLUB	*S*	(η^5-C_5H_5)Ru◁Ph_2PCH{CC=C(Ph)Me}CH_2PPh_2▷	[40]
KIGTID	*S,S*	Mo[Ph_2PCH(Ph)CH(Ph)PPh_2](CO)$_4$ · CH_2Cl_2	[41]
MPENFE	*S*	(η^5-C_5H_5)Fe◁Ph_2PCH{C=CMe_2}CH_2PPh_2▷	[42]
PNOBRH01	*R*	[(nbd)Rh{Ph_2PCH(C_6H_{11})CH_2PPh_2}][ClO_4]	[43]
PNOBRH02	*R*	[(nbd)Rh{Ph_2PCH(C_6H_{11})CH_2PPh_2}][ClO_4]	[43]
SOXHOC	*S*	{(*t*-butyl)CH_2}$_2$Pt{Ph_2PCH(Ph)CH_2PPh_2}	[44]
YIFCOF	*S*	[(η^5-C_5H_5)Fe{Ph_2PCH(CH=NH)CH_2PPh_2}]I · $CHCl_3 \cdot H_2O$	[45]

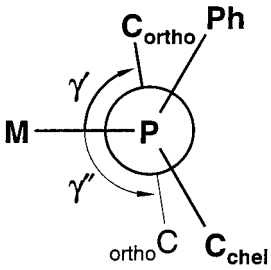

Fig. 4. Newman projection along the P–C_{ipso} bond. Definition of the phenyl orientation on the basis of the angles γ' and γ''.

As far as the rotation of the phenyl rings about the bond P–C_{ipso} is concerned there are the terms edge exposed and face exposed [6]. Viewed from the front side of a complex as in Fig. 1, a phenyl ring may expose its edge or its face to the neighboring coordination position at which the substrate to be transformed is bound. Although not well-defined [6], the terms edge exposed and face exposed have become fashionable in the recent literature [47–49]. In the present paper the angle γ (Fig. 4) is used as a measure to define the face–edge orientation of a phenyl ring. Small γ angles in the range between 0° and 45° indicate that C_{ortho} and its hydrogen atom are near to the metal center corresponding to an edge exposed orientation. Conversely, large γ values between 45° and 90° orient the π-electron cloud of the phenyl ring in the direction of the metal center, the phenyl ring having a face exposed character. As this differentiation is independent of the sign of γ, face or edge exposed phenyl rings may have either M chirality or P chirality, as defined in Fig. 5. Thus, the phenyl ring orientations can be subdivided into the four segments of 180°, to which the γ angle has been confined in Fig. 4: edge-P, edge-M, face-P and face-M orientation. In Fig. 5 a face-M orientation is shown. This definition allows a detailed discussion of the different phenyl arrangements.

In the following discussion, first the relation of the configuration of the asymmetric centers and the δ/λ-conformation of the complexes will be analyzed. An investigation as to the ring shapes according to conformational types I–III will follow. Then an analysis of M–P chirality and edge–face character of the phenyl orientations will be given. In addition, for those cases in which a clear differentiation between axial and equatorial phenyls is possible, a correlation to edge-P, edge-M, face-P and face-M will be made. These cases are both sides of the half-chair conformation (type I, Fig. 3a) and the 'steep' sides of the envelope conformations (types II and III, Fig. 3b,c).

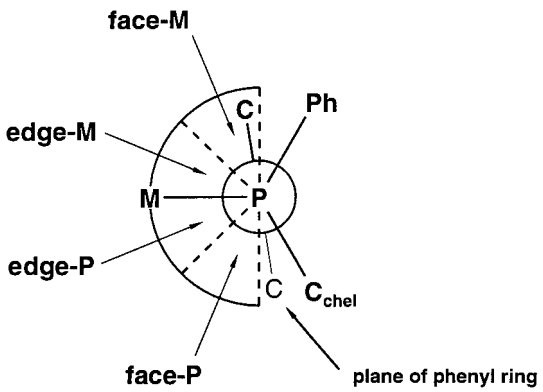

Fig. 5. Newman projection along the P–C_{ipso} bond. Definition of the sectors face-M, edge-M, edge-P and face-P.

3. Prophos complexes

With only one methyl substituent at the ethane bridge prophos is the simplest of the chiral bis(diphenylphosphanyl)ethane ligands. Table 2 shows the data of the 12 chelate rings of this phosphine in 10 of its crystal structures. The chirality of the chelate ring is, as expected [6,47–49], λ for (*R*)-prophos and δ for (*S*)-prophos, because the methyl group tends to be in an equatorial position. The only exception is the molecular structure COCONO (see Table 1 for code identification) [10]. In this compound, the methyl group of the phosphine ligand, surprisingly, is in an axial position, forcing the five-membered ring into the δ conformation, which is unusual for (*R*)-prophos. This is the more astonishing, as it cannot be induced by the additional ligands CO and NO, which are both linear and very similar.

The conformation of 6 of the chelate rings in Table 2 is envelope-like (type II, Fig. 3b). This conformation is characterized by a large α value (here torsion angle P2–M–P1–C_{chel}, α(P1)) and a much smaller α value with the same sign (here angle P1–M–P2–C_{chel}, α(P2)). In ligands with a λ chelate ring α(P1) and α(P2) have negative signs, in a δ chelate conformation they have positive signs (Table 2). Typical values of α(P1) and α(P2) in a type II envelope chelate ring of λ conformation are $-24°$ and $-1°$, respectively (see crystal structure GARZEE). As obvious from the picture of GARZEE in Table 2, the orientation of the prophos ligand in the back of the complex for all the entries in Table 2 is such that the asymmetric center is on the left-hand side concomitant with the large α angle also being on the left-hand side (exception FAXZIN).

In the type II category of chelate rings the asymmetric center is located at the 'steep' side of the envelope. This orientation allows the methyl substituent to point as horizontally as possible away from the complex. The envelope conformation causes the absolute values of β(Ph1) and β(Ph2) to be quite different, whereas, those of β(Ph3) and β(Ph4) are almost equal. As a consequence, in ligands with a λ chelate ring Ph1 is clearly equatorial and Ph2 is clearly axial, whereas, for Ph3 and Ph4 the differences between axial and equatorial posi-

Table 2
Data of prophos complexes

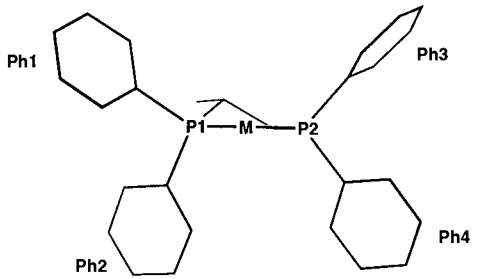

Complex	*R* / *S*	Ring	Conf.	P1	P2	Ph1				Ph2				Ph3				Ph4			
				α[°]	α[°]	β[°]	ax/eq	γ[°]	Orient.	β[°]	ax/eq	γ[°]	Orient.	β[°]	ax/eq	γ[°]	Orient.	β[°]	ax/eq	γ[°]	Orient.
BUHRIF10	*R*	λ	III	−30	8	−149	eq	−81,6	face-P	87	ax	−19,6	edge-P	129	eq	−3,9	edge-P	−111	ax	−74,4	face-P
BUHROL	*R*	λ	II	−18	−4	−140	eq	−67,7	face-P	98	ax	−38,3	edge-P	118	ax	32,7	edge-M	−122	eq	−80,6	face-P
COCONO	*R*	δ	II	16	7	−101	ax	−69,9	face-P	134	eq	−8,3	edge-P	123	eq	−62,6	face-P	−111	ax	−16,8	edge-P
FAXZIN	*R*	λ	I	−11	−14	−126	eq	34,9	edge-M	113	ax	67,2	face-M	103	ax	−31,6	edge−P	−135	eq	−59,8	face-P
FAXZOT	*R*	λ	II	−21	−1	−141	eq	−70,2	face-P	96	ax	−27,8	edge-P	118	ax	19,6	edge−M	−121	eq	−81,3	face-P
FUTWUM	*S*	δ	II	17	5	−99	ax	37,4	edge-M	139	eq	59,2	face-M	117		−29,7	edge-P	−117		−69,2	face-P
FUTXAT	*R*	λ	II	−23	−3	−138	eq	−78,8	face-P	94	ax	−37,6	edge-P	112	ax	−49,7	face-P	−123	eq	−57,5	face-P
	S	δ	II	16	6	−102	ax	51,8	face-M	138	eq	61,3	face-M	119	eq	−38,7	edge-P	−115	ax	−71,3	face-P
GARZEE	*R*	λ	II	−24	−1	−144	eq	−75,5	face-P	93	ax	−18,6	edge-P	121	eq	24,6	edge-M	−120	ax	82,4	face-M
LAWZEO	*R*	λ	I	−16	−8	−137	eq	−73,5	face-P	100	ax	−27,9	edge-P	112	ax	50,5	face-M	−127	eq	−81,2	face-P
	R	λ	III	−27	4	−148	eq	−70,3	face-P	89	ax	−20,6	edge-P	124	eq	31,1	edge-M	−116	ax	−86,7	face-P
LIFLER	*R*	λ	III	−33	9	−151	eq	88,9	face-M	83	ax	−20,0	edge-P	129	eq	3,9	edge-M	−109	ax	−50,8	face-P

The picture shows the chelate ring of complex GARZEE as an example.

tion are only small. Typical values are −144° and 93° for β(Ph1) and β(Ph2) compared to 121° and −120° for β(Ph3) and β(Ph4) of the chelate ring in GARZEE. In complexes with a δ chelate ring the situation is the other way round.

A half-chair conformation (type I, Fig. 3a) is found in the (*R*)-prophos complexes COCONO, LAWZEO (only the first ligand) and almost ideally in the crystal structure FAXZIN (α(P1) = −11° and α(P2) = −14°). The half-chair conformation leads to a clear axial–equatorial distinction of Ph2 and Ph1 as well as Ph3 and Ph4, respectively, e.g., β(Ph2) = 113°/β(Ph1) = −126° and β(Ph3) = 103°/β(Ph4) = −135° in crystal structure FAXZIN.

Values of α with different signs—BUHRIF10, LAWZEO (second ligand) and LIFLER—result in a distorted envelope conformation (type III, Fig. 3c), accompanied by the expected inversion of the axial–equatorial positions of Ph3 and Ph4 compared to the envelope chelate rings discussed above.

The coupling of the two α angles α(P1) and α(P2) to each other by the rigid five-membered ring system is indicated by the constant sum |α(P1) + α(P2)|, which is between 22° and 26° for all the prophos complexes in Table 2.

An analysis of the chirality of the phenyl ring orientation in the 10 chelate rings of (*R*)-prophos in Table 2 according to Fig. 5 allows a subdivision into three groups: (i) In 3 cases all 4 phenyl rings have P chirality (P^4), (ii) In 4 cases 3 rings have P chirality and 1 ring has M chirality (P^3M), (iii) In 3 cases 2 rings have P and 2 M chirality (P^2M^2). Combinations with more than 2 rings having M chirality (PM^3, M^4) are not observed. This result shows, that there is a chiral induction from the asymmetric center on the orientation of the phenyl rings: (*R*)-prophos promotes predominantly P chirality. This also holds for the crystal structure COCONO. Although the chelate ring is inverted compared to other (*R*)-prophos complexes, the phenyl rings of the ligand show a P^4 chirality pattern. For (*S*)-prophos only 2 complexes were retrieved and analyzed (Table 2). In both cases, 2 phenyl rings have M and 2 have P chirality (M^2P^2).

Similar to P and M chirality certain orientations are preferred with respect to edge and face exposure. In 9 out of 10 (*R*)-prophos ligands Ph1 is face exposed, while Ph2 is edge exposed and in 7 out of these 10 ligands Ph4 is face exposed, while Ph3 is edge exposed. Also, a correlation of face–edge exposure and P–M chirality of the phenyl orientations is observed (Fig. 5). In the (*R*)-prophos complexes the orientation of Ph1 is predominantly face-P (8 out of 10 ligands). Ph2 is found in edge-P orientation in 9 of 10 cases. In 5 ligands Ph3 is in an edge-M and in 8 ligands Ph4 is in a face-P position. In the 2 (*S*)-prophos complexes Ph1 is in an edge-M and face-M position, respectively, whereas, both Ph2 rings are in a face-M conformation. The phenyls Ph3 have both edge-P and Ph4 both face-P orientation.

Relating edge and face exposure with the axial or equatorial arrangement of phenyl rings bonded at P1 (large α angle) shows that axial phenyls are preferably edge exposed, whereas, equatorial phenyls are mainly face exposed. In nearly all ligands with *R* chirality making a λ chelate ring, this preference can be seen. Only the crystal structure FAXZIN is an exception. The complex BUHROL is a typical example. The γ values are −67.7° for Ph1 (eq, face-P), −38.3° for Ph2 (ax, edge-P), 32.7° (ax, edge-M) and −80.6° (eq, face-P). This example also shows the dominance of P chirality in phenyl ring orientation.

On the P2 side of the prophos complexes, except for the half-chair complex FAXZIN, the α angles generally are small ('flat' envelope side). As a consequence, there is a strongly reduced axial–equatorial differentiation of Ph3 and Ph4. Nevertheless, most of the complexes reveal a M–P and edge–face selectivity, which probably is due to a transfer from the more differentiated other side of the chelate ring.

4. Chiraphos complexes

Compared to prophos, the ligand chiraphos contains an additional methyl group and thus another chiral center. The angles of 11 complexed ligands are listed in Table 3. Only crystal structures with (2*S*,3*S*)-chiraphos were found in the CSD. In all of them the chelate ring is in the expected δ conformation.

6 of the 11 chelate rings are in the distorted envelope conformation (type III), a conformation which is relatively rare for prophos complexes. A typical example is the crystal structure DUBTUP with α values (first ligand) of 32° (P1) and −14° (P2). Ph1 and Ph3 therefore are clearly axial, Ph2 and Ph4 clearly equatorial. With α(P2) values of −1° the chelate rings of complexes SAZTAO and PODDAN are near the borderline to the type II envelope conformation.

Only 2 ligands out of 11 show the type II envelope chelate ring conformation (SAZTES, SAHNEU second ligand), which dominated in the series of the prophos complexes. In SAZTES, the high α(P1) value of 26° causes a clear differentiation of the axial and equatorial phenyl rings Ph1 (β −90°) and Ph2 (β 146°), respectively. The axial–equatorial arrangement of the two phenyls at P2 is not as expected. The β values are 117° and −120° for Ph3 and Ph4, respectively, due to a distortion at the P2 atom.

3 chelate rings can be described as type I half-chair (CUYYAW, SAHNEU first ligand, OCPBRH). The crystal structure OCPBRH contains a nearly symmetrical chelate ring with α values of 15° and 12°. Also the

Table 3
Data of chiraphos complexes

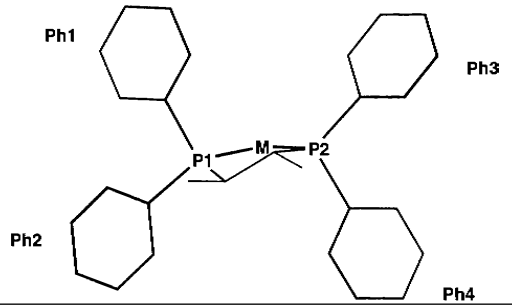

Complex	*R*/*S*	Ring Conf.		P1	P2	Ph1				Ph2				Ph3				Ph4			
				α[°]	α[°]	β[°]	ax/eq	γ[°]	Orient.	β[°]	ax/eq	γ[°]	Orient.	β[°]	ax/eq	γ[°]	Orient.	β[°]	ax/eq	γ[°]	Orient.
CUYYAW	*S*,*S*	δ	II	15	6	−100	ax	12,7	edge-M	139	eq	87,6	face-M	131	eq	81,2	face-M	−105	ax	30,5	edge-M
DOCPIU	*S*,*S*	δ	III	25	−8	−94	ax	39,2	edge-M	142	eq	71,2	face-M	110	ax	68,2	face-M	−135	eq	8,4	edge-M
	S,*S*	δ	III	32	−15	−87	ax	28,5	edge-M	149	eq	86,0	face-M	105	ax	71,8	face-M	−140	eq	15,6	edge-M
DUBTUP	*S*,*S*	δ	III	32	−14	−87	ax	−13,0	edge-P	147	eq	−64,5	face-P	97	ax	9,0	edge-M	−138	eq	60,0	face-M
	S,*S*	δ	III	33	−13	−84	ax	−9,0	edge-P	150	eq	−73,0	face-P	99	ax	7,5	edge-M	−136	eq	63,0	face-M
OCPBRH	*S*,*S*	δ	I	15	12	−103	ax	8,1	edge-M	135	eq	−70,8	face-P	132	eq	−70,3	face-P	−106	ax	10,0	edge-M
PODDAN	*S*,*S*	δ	III	27	−1	−86	ax	13,7	edge-M	147	eq	83,6	face-M	118	ax	88,5	face-M	−119	eq	25,9	edge-M
SAHNEU	*S*,*S*	δ	I	14	9	−111	ax	−70,3	face-P	128	eq	58,4	face-M	126	eq	74,5	face-M	−103	ax	30,6	edge-M
	S,*S*	δ	II	19	4	−107	ax	−67,3	face-P	132	eq	−29,9	edge-P	125	eq	61,1	face-M	−110	ax	37,3	edge-M
SAZTAO	*S*,*S*	δ	III	28	−1	−88	ax	13,1	edge-M	147	eq	87,8	face-M	115	ax	89,3	face-M	−123	eq	16,8	edge-M
SAZTES	*S*,*S*	δ	II	26	2	−90	ax	21,5	edge-M	146	eq	83,0	face-M	117	ax	79,4	face-M	−120	eq	41,3	edge-M

The picture shows the chelate ring of complex CUYYAW as an example.

Table 4
Data of norphos (upper part) and renorphos (lower part) complexes

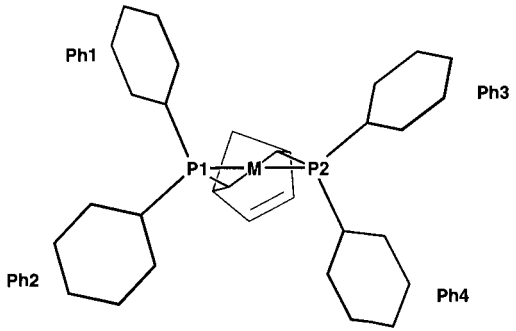

Complex	*R*/*S*	Ring	Conf.	P1	P2	Ph1				Ph2				Ph3				Ph4			
				α[°]	α[°]	β[°]	ax/eq	γ[°]	Orient.	β[°]	ax/eq	γ[°]	Orient.	β[°]	ax/eq	γ[°]	Orient.	β[°]	ax/eq	γ[°]	Orient.
BAVSAS	*S,S*	δ	I	15	14	−100	ax	−7,4	edge-P	133	eq	−43,1	edge-P	135	eq	63,5	face-M	−104	ax	6,3	edge-M
CICPEJ	*R,R*	λ	I	−16	−15	−130	eq	−74,3	face-P	103	ax	−25,7	edge-P	106	ax	30,7	edge-M	−127	eq	55,0	face-M
HATJOB	*R,R*	λ	I	−12	−19	−133	eq	−87,1	face-P	104	ax	−12,0	edge-P	102	ax	−4,9	edge-P	−133	eq	61,1	face-M
VIMBEY	*R,R*	λ	I	−18	−10	−137	eq	−65,0	face-P	99	ax	−22,2	edge-P	115	ax	36,9	edge-M	−121	eq	62,0	face-M
Complex	*R*/*S*	Ring	Conf.	P1	P2	Ph1				Ph2				Ph3				Ph4			
				α[°]	α[°]	β[°]	ax/eq	γ[°]	Orient.	β[°]	ax/eq	γ[°]	Orient.	β[°]	ax/eq	γ[°]	Orient.	β[°]	ax/eq	γ[°]	Orient.
CEJJEG	*R,R*	λ	I	−14	−15	−134	eq	−65,6	face-P	105	ax	−9,6	edge-P	101	ax	6,4	edge-M	−132	eq	44,2	edge-M
CUNKUR	*S,S*	δ	I	17	11	−98	ax	2,0	edge-M	132	eq	70,0	face-M	127	eq	85,8	face-M	−107	ax	11,0	edge-M
DIRE	*S,S*	δ	I	14	15	−95	ax	12,2	edge-M	129	eq	66,2	face-M	129	eq	69,5	face-M	−100	ax	17,3	edge-M
	S,S	δ	I	14	15	−100	ax	17,1	edge-M	126	eq	65,8	face-M	129	eq	65,4	face-M	−101	ax	11,9	edge-M

The picture shows the chelate ring of complex BAVSAS as an example.

β values are nearly equal with $-103°$ and $-106°$ for the axial and 135° and 132° for the equatorial phenyl rings.

In the chiraphos complexes the sum $|\alpha(P1) + \alpha(P2)|$ varies in the range from 17° to 27°, appreciably more than in the prophos complexes.

A M/P analysis of the phenyl ring orientations shows that M chirality is preferred. In 6 cases, all 4 phenyl rings have M chirality (M^4); in 1 case we find the M^3P and in 4 cases the M^2P^2 chirality pattern. This shows, that (*S,S*)-chiraphos promotes M chirality in the orientation of the phenyl rings. The somewhat higher selectivity, compared to prophos complexes, may be caused by the 'double' chiral information in the ligand backbone.

In 9 of the 11 (*S,S*)-chiraphos complexes Ph1 is edge exposed, whereas Ph2 is face exposed. This is in accord with the results obtained for the (*R*)-prophos complexes, taking into account that in (*R*)-prophos the inducing chirality is inverted with respect to (*S,S*)-chiraphos. In 9 of 11 chiraphos complexes Ph3 is face exposed, whereas Ph4 is edge exposed. This, however, is different to the prophos situation.

In 6 (*S,S*)-chiraphos ligands both of the phenyls bonded at P1 and in 10 (*S,S*)-chiraphos ligands both of the phenyls bonded at P2 have M chirality. Without exception, when the phenyl chirality is M, Ph1 and Ph4 are edge exposed, whilst Ph2 and Ph3 are face exposed.

For the phenyl rings bonded at P1, in 9 of 11 cases the axial Ph1 is edge exposed, whereas the equatorial Ph2 is face exposed. The situation at P2 is not as clear-cut due to the less pronounced chelate ring puckering. Only in complexes with a half-chair or a clear distorted envelope conformation a correlation between axial–equatorial and face–edge exposed is possible.

5. Norphos and renorphos complexes

Due to the rigid skeleton of the ligands, the chelate rings in complexes containing norphos or renorphos are more rigid than in the prophos and chiraphos complexes (Table 4).

The chirality of the 8 chelate rings is as expected δ for *S,S* ligands and λ for *R,R* ligands. The α angles are very similar as all the chelate rings have the half chair conformation, causing the sum $\alpha(P1) + \alpha(P2)$ to be quite constant between 28° and 31°. As a consequence there is a clear axial and equatorial differentiation of the phenyl rings. The β values are in the close range between 95° (DIRE) and 107° (CUNKUR) for axial phenyls as well as 126° (DIRE) and 137° (VIMBEY) for equatorial phenyls. Only the phenyls bonded to P2 in crystal structure VIMBEY are not within this range.

4 of the 8 ligands show a selectivity in the chirality of the phenyl ring orientation: 3 (*S,S*)-renorphos chelates with M^4-chirality (CUNKUR, DIRE) and 1 (*R,R*)-norphos complex with P^3M-chirality (HATJOB). The other 4 chelate rings follow the M^2P^2 chirality pattern.

Due to the well behaved chelate ring puckering the interdependence of edge and face exposure of the phenyl rings and their axial and equatorial positions is obvious. All 16 axial phenyl rings are edge exposed, whilst 15 of 16 equatorial phenyl rings are face exposed. The phenyl ring deviating is Ph2 in crystal structure BAVSAS with a γ angle of $-43{,}1°$. Thus, in the norphos and renorphos crystal structures, the selectivity for the sectors defining the edge–face character of the phenyl rings is much higher than the selectivity for the sectors defining the M–P character (Fig. 5).

6. Complexes with chiral cyclic phosphines

The data of complexes containing cyclic phosphines which form five-membered rings are compiled in Table 5. In all of them, the diphenylphosphanyl groups are in trans-1,2-positions of a ring which forms the common structural element of this class of compounds. In most cases these rings are carbocyclic (BUTWES, HAJKUJ, SOSPEV, FECDIA), in two cases the rings are heterocyclic (SACHIN, CASDOP).

The chirality of the chelate ring conformations is as expected (δ for *S,S* configuration and λ for *R,R* configuration at the 1,2 ring positions). Obviously, this correlation is reinforced by the cyclic structure fused to the five-membered chelate ring.

In this group of complexes, most of the chelate ring conformations can be described as a half chair (BUTWES, FECDIA, SACHIN, both rings of SOSPEV). A typical example is the crystal structure SOSPEV with α values of $-14°$ and $-12°$ for one ring and 14° and 12° for the other. In complex HAJKUJ both chelate rings are in envelope conformations with α values of 25° and 0° or $-25°$ and 0° causing the $|\beta|$ values of Ph3 and Ph4 to be nearly equal (116° and 113°), whereas the $|\beta|$ values of Ph1 and Ph2 are quite different (141° and 89° in both rings). Only in crystal structure CASDOP the chelate ring forms a distorted envelope with $\alpha(P1)$ and $\alpha(P2)$ having different signs. In this molecular structure a rigid carboxylic acid anhydride moiety is part of the ring fused to the five-membered chelate system. The α values reach 37° and $-23°$. The consequence is the extremely axial character of Ph1 and Ph3 and the equatorial character of Ph2 and Ph4 evident from the picture below Table 5. The rigid two-ring-structures of all these complexes cause the sum of $\alpha(P1)$ and $\alpha(P2)$ to be relatively constant between 25° and 27° (exception CASDOP).

An analysis of the torsion angles of the phenyl rings shows that one (*R,R*)-phosphine ligand has P^4 chirality

Table 5
Data of cyclic phosphines. The picture shows the chelate ring of complex BUTWES as an example. The substitution patterns are explained below.

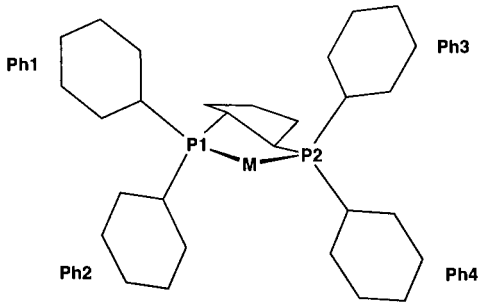

Complex	*R*/*S*	Ring	Conf.	P1	P2	Ph1				Ph2				Ph3				Ph4			
				α[°]	α[°]	β[°]	ax/eq	γ[°]	Orient.	β[°]	ax/eq	γ[°]	Orient.	β[°]	ax/eq	γ[°]	Orient.	β[°]	ax/eq	γ[°]	Orient.
BUTWES	*R*,*R*	λ	I	−18	−9	−138	eq	−74,8	face-P	96	ax	−14,1	edge-P	107	ax	−16,9	edge-P	−126	eq	82,4	face-M
CASDOP	*S*,*S*	δ	III	37	−23	−76	ax	−53,7	face-P	163	eq	−41,6	edge-P	91	ax	14,0	edge-M	−140	eq	36,0	edge-M
FECDIA	*R*,*R*	λ	I	−11	−16	−128	eq	−30,6	edge-P	105	ax	2,2	edge-M	99	ax	−3,0	edge-P	−135	eq	79,3	face-M
HAJKUJ	*S*,*S*	δ	II	25	0	−89	ax	8,3	edge-M	141	eq	−87,5	face-P	113	ax	1,9	edge-M	−116	eq	46,9	face-M
	R,*R*	λ	II	−25	0	−141	eq	87,5	face-M	89	ax	−8,3	edge-P	116	eq	−46,8	face-P	−113	ax	−1,9	edge-P
SACHIN	*R*,*R*	λ	I	−14	−12	−132	eq	−83,6	face-P	103	ax	−10,0	edge-P	102	ax	−19,6	edge-P	−137	eq	−71,5	face-P
SOSPEV	*R*,*R*	λ	I	−14	−12	−129	eq	54,3	face-M	102	ax	67,8	face-M	103	ax	−18,7	edge-P	−125	eq	−87,5	face-P
	S,*S*	δ	I	14	12	−102	ax	−67,8	face-P	129	eq	−54,3	face-P	125	eq	87,5	face-M	103	ax	18,7	edge-M

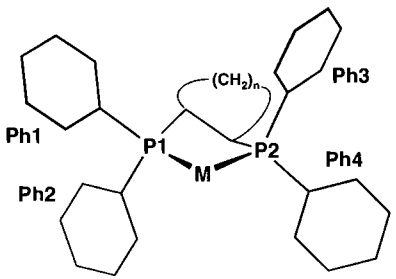

n=3 BUTWES, HAJKUJ, SOSPEV
n=2 FECDIA

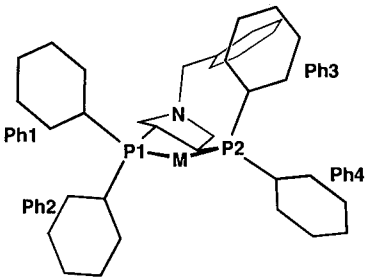

SACHIN

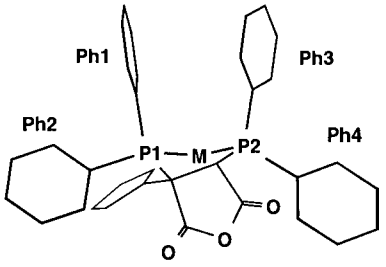

CASDOP

Table 6
Data of complexes with various phosphines

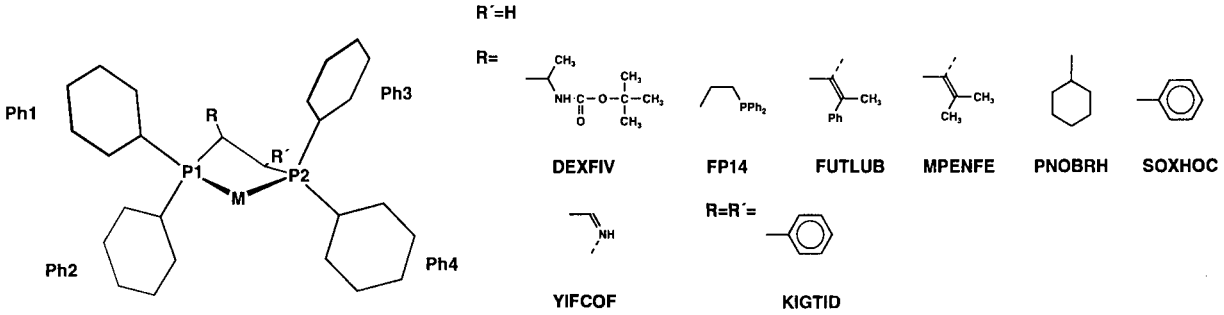

Complex	*R*/*S*	Ring	Conf.	P1	P2	Ph1				Ph2				Ph3				Ph4			
				α[°]	α[°]	β[°]	ax/eq	γ[°]	Orient.	β[°]	ax/eq	γ[°]	Orient.	β[°]	ax/eq	γ[°]	Orient.	β[°]	ax/eq	γ[°]	Orient.
DEXFIV	*R*	λ	III	−27	2	−144	eq	−77,7	face-P	89	ax	−30,9	edge-P	117	eq	76,5	face-M	−113	ax	18,6	edge-M
	R	λ	III	−27	2	−144	eq	−77,7	face-P	89	ax	−30,9	edge-P	117	eq	76,5	face-M	−113	ax	18,6	edge-M
FP14	*R*	λ	I	−14	−7	−135	eq	−64,5	face-P	101	ax	−26,8	edge-P	110	ax	75,1	face-M	−124	eq	14,5	edge-M
FUTLUB	*S*	λ	III	−49	27	−158	eq	−80,1	face-P	64	ax	22,8	edge-M	140	eq	6,3	edge-M	−96	ax	−79,0	face-P
KIGTID	*S*,*S*	δ	III	27	−2	−93	ax	24,0	edge-M	143	eq	−85,2	face-P	115	ax	81,4	face-M	−125	eq	28,7	edge-M
MPENFE	*S*	λ	III	−51	31	−161	eq	78,4	face-M	63	ax	36,8	edge-M	147	eq	−7,4	edge-P	−89	ax	−75,5	face-P
PNOBRH01	*R*	λ	I	−8	−7	−134	eq	−85,5	face-P	107	ax	−14,1	edge-P	114	ax	75,4	face-M	−125	eq	27,3	edge-M
	R	λ	II	−3	−22	−126	eq	−67,2	face-P	114	ax	−26,1	edge-P	95	ax	28,2	edge-M	−135	eq	52,3	face-M
PNOBRH02	*R*	λ	I	−14	−11	−136	eq	−67,9	face-P	104	ax	−24,0	edge-P	105	ax	67,1	face-M	−127	eq	3,0	edge-M
SOXHOC	*S*	δ	III	30	−6	−82	ax	5,7	edge-M	144	eq	−55,3	face-P	107	ax	12,5	edge-M	−128	eq	81,7	face-M
YIFCOF	*S*	λ	III	−45	23	−153	eq	3,0	edge-M	71	ax	46,6	face-M	137	eq	17,0	edge-M	−96	ax	60,6	face-M

The picture shows a common view at the chelate ring and the substituents of each ligand.

Table 7
(*R*)- and (*R,R*)-ligands and their phenyl ring chirality

Chirality	Prophos	Chiraphos	Norphos/renorphos	Cyclic phosphines	Various phosphines	
P^4	3	–	0	1	0	4
P^3M	4	–	1	2	0	7
P^2M^2	3	–	3	2	6	14
	10	–	4	5	6	25

(SACHIN), two have P^3M chirality (HAJKUJ second ligand, BUTWES). One (*S,S*)-phosphine ligand leads to a M^3P conformation (HAJKUJ first ligand). The other 4 ligands have M^2P^2 chirality. In the P^4 complex SACHIN, which has a λ chelate ring in a half chair conformation, the axial phenyls Ph2 and Ph3 are clearly edge exposed with γ values of $-10{,}0°$ for Ph2 and $-19{,}6°$ for Ph3, whereas the equatorial phenyls are face exposed (γ values of $-83{,}6°$ for Ph1 and $-71{,}5°$ for Ph4).

All the phenyl rings with a clear axial and equatorial character are analyzed with respect to a correlation with edge–face exposure. In complexes with envelope conformations of the chelate rings only phenyl pairs at the 'steep side', in complexes with half chair chelate rings all phenyls are taken into consideration. 10 of 12 axial phenyl rings are edge exposed and 11 of 12 equatorial phenyl rings are face exposed. This analysis proofs, that axial phenyl rings prefer an edge exposed arrangement, whilst the equatorial ones prefer a face exposed arrangement. The exceptional complex CASDOP with a distorted envelope chelate ring has 3 edge exposed phenyl rings and 1 face exposed phenyl ring.

7. Other complexes containing five-membered chelate rings with chiral PP ligands

The data of complexes containing chelate ligands with various substituents at the two-carbon bridge between the two diphenylphosphanyl groups are shown in Table 6. As all these compounds lack a common structural element in the ligand backbone, they cannot be easily compared.

The correlation inducing chirality → chelate ring conformation ($S \rightarrow \delta$ or $R \rightarrow \lambda$) is valid as in the previous chapters, except for crystal structures YIFCOF, FUTLUB and MPENFE, the chelate rings of which are inverted. The reason for this inversion is the coordination of one of their substituents at the backbone to the metal atom, forcing it into an axial position.

In 3 cases out of 11 the chelate ring is half chair-like (PNOBRH02, PNOBRH01 first ligand, FP14). A typical example is the complex PNOBRH02 with α(P1) and α(P2) values of $-14°$ and $-11°$. The λ chirality of the chelate ring causes Ph1 and Ph4 to be clearly equatorial with β values of $-136°$ and $-127°$, whereas Ph2 and Ph3 are in axial positions having β values of 104° and 105°, respectively. The second ligand of PNOBRH01 has the envelope conformation and 7 chelate rings are in the distorted envelope conformation with α(P1) and α(P2) having different signs [DEXFIV (both rings), FUTLUB, KIGTID, MPENFE, SOXHOC, YIFCOF]. An example for an extremely distorted envelope is crystal structure MPENFE with α values of $-51°$ and 31° (λ conformation). As a consequence, the β angles of Ph1 and Ph2 are very different from each other ($-161°$ and 63°). This unusual conformation is induced by the metal coordination of the additional olefinic double bond. The other complexes with coordinating third substituents at the phosphine ligand (YIFCOF, FUTLUB) have similar conformations.

An analysis of the chirality of the phenyl ring orientation reveals that the selectivity is low compared to other ligand groups. Only 1 (*S*)-phosphine ligand has M^4 chirality (YIFCOF), 2 have M^3P-chirality (KIGTID, SOXHOC), whereas the other 8 ligands have M^2P^2 chirality.

In the correlation axial–equatorial character vs. edge–face exposure of the phenyl rings of half chair conformations and the phenyl pairs of the 'steep' sides of envelope conformations no selectivity is found. 4 of 7 axial phenyl rings are edge exposed, the others face exposed and 4 of 7 equatorial phenyl rings are face exposed, the others edge exposed.

In ligands with distorted envelope chelate rings of

Table 8
(*S*)- and (*S,S*)-ligands and their phenyl ring chirality

Chirality	Prophos	Chiraphos	Norphos	Cyclic phosphines	Various phosphines	
M^4	0	6	3	0	1	10
M^3P	0	1	0	1	2	4
M^2P^2	2	4	1	2	2	11
	2	11	4	3	5	25

type III (Fig. 3c) the axial and equatorial character of the phenyls at P2 (the larger γ angle is always at P1) is inverted compared to type I and type II ligands. Therefore, the phenyl pairs of P1 ('steep' side) and P2 ('flat' side) are analyzed separately. At P1, 6 of 7 axial phenyls are edge exposed, and 6 of 7 equatorial phenyls are face exposed. The results for the 7 phenyl pairs at P2 are different. 3 axial phenyls are edge exposed, 4 are face exposed and 3 equatorial phenyls are face exposed, 4 are edge exposed. Thus, in complexes with a distorted

Table 9
CSD reference codes and formulas of all analyzed diphos compounds

Ref. code	Formula	Ref.
BAYGEN	$Ru(diphos)(PhCSO)_2(PPhMe_2) \cdot CH_3OH$	[50]
BUCKAL	$\{Rh(diphos)(\mu\text{-}PPh_2)\}_2 \cdot THF$	[51]
CASYAW	$[Ru(diphos)_2(HC{=}O)CO][SbF_6] \cdot CH_2Cl_2$	[52]
CODTEU10	$Rh(diphos)(C_7H_7)Fe(CO)_3$	[53]
CULWIP	$[Rh(diphos)(\mu\text{-}H)(\mu\text{-}Cl)IrCl(PEt_3)_3][BF_4]$	[54]
CULWOV	$[Rh(diphos)(\mu\text{-}H)(\mu\text{-}Cl)IrH(PEt_3)_3][BF_4]$	[54]
CUNMED	$(\eta^5\text{-}C_5H_5)Ru(diphos(\{C[{=}C(CN)_2]C(Ph){=}C(CN)_2\} \cdot 0{,}5\ CHCl_3$	[55]
DAJGEA	$[(\eta^5\text{-}C_5H_5)(PPh_3)_2Ru(\eta\text{-}CN)Ru(diphos)(\eta^5\text{-}C_5H_5)][PF_6]$	[56]
DOBPOZ	$[(\eta^5\text{-}C_5H_5)Ru(diphos)\{C{=}CPh(C_7H_7)\}][PF_6] \cdot 0{,}63\ CH_2Cl_2$	[57]
DPERUB10	$[Ru(diphos)_2NO][BPh_4] \cdot MeCOMe$	[58]
DUJXIP	$[Rh(diphos)_2][Ag\{C(CF_3)_2F\}_2]$	[59]
DUMZIU	$H_3Ru_3Co(CO)_{10}(diphos)$	[60]
FAWHOA	$(\eta^5\text{-}C_5H_5)Ru(diphos)\{C[{=}C(CN)_2]C(Ph){=}CH(C_6H_4NO_2)\} \cdot 0{,}5\ CH_2Cl_2$	[61]
FIRZOV	$(\eta^5\text{-}C_5H_5)Ru(diphos)(C{\equiv}CPh)$	[62]
FUVPER	$(\eta^5\text{-}C_5H_5)Ru(diphos)\{C(CO_2Me){=}CH(CO_2Me)\}$	[63]
GECLAB	$[Ru_2(CO)_4(diphos)_2(\mu\text{-}O_2CMe)][PF_6]$	[64]
HACVOW	$(\eta^5\text{-}C_5H_5)Ru(diphos)Cl \cdot CDCl_3$	[65]
HACVOW01	$(\eta^5\text{-}C_5H_5)Ru(diphos)Cl \cdot CHCl_3$	[66]
JIJFAJ	$RhH(diphos)_2$	[67]
KICZUR	$Ru(diphos)_2Cl_2 \cdot CH_2Cl_2$	[68]
KOMPAD	$(\eta^5\text{-}C_5H_4Me)Ru(diphos)(SReS_3) \cdot Et_2O$	[69]
KUFLUS	$Ru_8Pt_2(CO)_{23}(diphos)(\mu\text{-}H)_2 \cdot 0{,}75\ CH_2Cl_2$	[70]
KURROE	$[Rh_2(diphos)(bpy)(\mu\text{-}CO)\{\mu\text{-}(p\text{-tolyl})NNN(p\text{-tolyl})\}_2][PF_6] \cdot 0{,}67\ C_6H_{14} \cdot H_2O$	[71]
LEHZON	$[(\eta^5\text{-}C_5Me_5)Ir(\mu\text{-}pz)_3Rh(diphos)(OOH)][BF_4]$	[72]
LEMLOE	$[\{C_5H_4(neomenthyl)\}Ru(diphos)(IEt)][CF_3SO_3]$	[73]
NABBEX	$Ru(diphos)\{C{\equiv}CC_6H_3(NO_2)Me\}Cl$	[74]
PAFFOR	$[(\eta^5\text{-}C_5H_5)Ru(diphos)(S{=}CHC_6H_4OMe)][PF_6] \cdot 0{,}5\ Et_2O$	[75]
PAFPAN	$[Rh_2(form)(O_2CCF_3)(diphos)\{(C_6H_4)PhPCH_2CH_2PPh_2\}][CF_3COO] \cdot 0{,}5\ H_2O$ form = *N*,*N*′-di-*p*-tolylformamidinate anion	[76]
PERUHC10	$Ru_4(\mu\text{-}H)_4(CO)_{10}(diphos)$	[77]
PHETHB	$Rh(diphos)(\eta\text{-}BPh_4)$	[78]
PIRKAC	$[Ru(diphos)_2(C{\equiv}CPh)NH_3][PF_6]$	[79]
POGNEE	$Ru(diphos)_2Cl_2$	[80]
POGNII	$[Ru(diphos)_2Cl][BF_4]$	[80]
PPERHC	$[Rh(diphos)_2][ClO_4]$	[81]
RHEPPO10	$[Rh(O_2)(diphos)_2][PF_6]$	[82]
SOZTEG	$[Rh(diphos)(imine)_2][BF_4] \cdot CH_2Cl_2 \cdot H_2O$ imine = 6,7-dimethoxy-1-methyl-3,4-dihydroisoquinoline	[83]
SUKSIA	$[(\eta^5\text{-}C_5Me_5)Ru(diphos)(O_2)][PF_6]$	[84]
VIMGIH	$Ru(diphos)(SC_5H_4N)_2$	[85]
VIRFEH	$Ru(diphos)(CO)_2[CON(C_6H_4Cl)O]$	[86]
VOLTIZ	$\{Rh(diphos)Cl\}_2(\mu\text{-}Cl)_2(\mu\text{-}CH_2)$	[87]
WEHHIA	$Ru(diphos)_2(C{\equiv}CPh)_2$	[88]
WELVUE	$Ru(diphos)(CO)_2(CONHCHMe_2)_2 \cdot 0{,}5\ C_6D_6$	[89]
WELWAL	$Ru(diphos)(CO)(NH_2CH_2Ph)[CONHCH_2Ph]_2$	[89]
WINJIM	$Rh(diphos)(B_9H_{10}S) \cdot 2\ CH_2Cl_2$	[90]
YEPSAN	$Ru(diphos)_2(C{\equiv}CPh)Cl \cdot CH_2Cl_2$	[91]
YETHUA	$[Ru(diphos)_2(C{=}C{=}C{=}CPh_2)Cl][PF_6] \cdot CH_2Cl_2$	[92]
YEXZEG	$[Ru(diphos)_2Cl][PF_6]$	[93]
YEXZIK	$[RuH_2(diphos)_2Cl][PF_6]$	[93]
YIDTAG	$Ru(diphos)(CO)_2\{\eta^2\text{-}ONC_6H_3(Cl)CF_3\} \cdot CH_2Cl_2$	[94]
YOYYUG	$[Rh(diphos)_2Cl_2]Cl \cdot EtOH$	[95]
ZIPVAV	$[(\eta^5\text{-}C_5Me_5)Ru(diphos)Cl_2][CF_3SO_3] \cdot 2\ CH_3NO_2$	[96]
ZIPVEZ	$[(\eta^5\text{-}C_5Me_5)Ru(diphos)NO][CF_3SO_3]_2 \cdot CH_3NO_2$	[96]

Table 10
Data of diphos complexes with a δ chelate ring (larger α angle at P1)

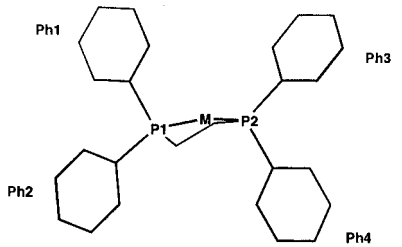

Complex	Ring	Conf.	P1	P2	Ph1				Ph2				Ph3				Ph4			
			α[°]	α[°]	β[°]	ax/eq	γ[°]	Orient.	β[°]	ax/eq	γ[°]	Orient.	β[°]	ax/eq	γ[°]	Orient.	β[°]	ax/eq	γ[°]	Orient.
BUCKAL	δ	III	27	−7	−85	ax	9,3	edge-M	143	eq	−82,0	face-P	108	ax	2,2	edge-M	−126	eq	68,2	face-M
CASYAW	δ	III	29	−7	−90	ax	−39,7	edge-P	139	eq	−77,0	face-P	105	ax	31,1	edge-M	−130	eq	79,3	face-M
CODTEU10	δ	I	13	11	−105	ax	20,6	edge-M	130	eq	40,2	edge-M	126	eq	−64,4	face-P	−112	ax	−31,0	edge-P
CULWOV	δ	II	17	7	−98	ax	22,5	edge-M	139	eq	69,6	face-M	126	eq	16,3	edge-M	−112	ax	−63,1	face-P
DPERUB10	δ	III	26	−4	−87	ax	−7,4	edge-P	148	eq	81,9	face-M	113	ax	−77,1	face-P	−127	eq	−40,8	edge-P
FAWHOA	δ	II	20	4	−92	ax	31,3	edge-M	146	eq	61,0	face-M	120	eq	50,8	face-M	−115	ax	59,7	face-M
FIRZOV	δ	III	29	−16	−90	ax	−63,4	face-P	147	eq	2,8	edge-M	103	ax	−87,8	face-P	−138	eq	−3,5	edge-P
FUVPER	δ	I	8	5	−118	ax	−15,2	edge-P	123	eq	−78,2	face-P	129	eq	18,4	edge-M	−112	ax	84,2	face-M
HACVOW	δ	II	22	3	−95	ax	12,9	edge-M	143	eq	58,6	face-M	120	eq	−76,0	face-P	−118	ax	−14,8	edge-P
KICZUR	δ	III	31	−10	−85	ax	−56,5	face-P	148	eq	−41,2	edge-P	104	ax	−35,8	edge-P	−127	eq	88,6	face-M

KUFLUS	δ	II	17	6	−101	ax	−51,4	face-P	136	eq	48,9	face-M	122	eq	−53,4	face-P	−115	ax	−62,0	face-P
LEMLOE	δ	II	18	7	−99	ax	25,2	edge-M	135	eq	54,9	face-M	125	eq	−47,1	face-P	−109	ax	−62,6	face-P
NABBEX	δ	III	28	−4	−89	ax	−56,0	face-P	143	eq	−25,3	edge-P	111	ax	−61,4	face-P	−122	eq	−36,9	edge-P
PAFFOR	δ	I	16	8	−101	ax	22,9	edge-M	136	eq	57,2	face-M	125	eq	−51,8	face-P	−111	ax	−59,2	face-P
PAFPAN[a]	δ	II	15	4	−95	ax	−57,5	face-P	157	eq	17,4	edge-M	121	eq	−79,5	face-P	−115	ax	−1,8	edge-P
PHETHB	δ	II	23	2	−92	ax	26,5	edge-M	142	eq	79,1	face-M	123	eq	−24,2	edge-P	−115	ax	−71,4	face-P
PIRKAC	δ	III	31	−24	−86	ax	−51,5	face-P	146	eq	−46,5	face-P	93	ax	84,5	face-M	−143	eq	1,9	edge-M
POGNEE	δ	III	32	−10	−80	ax	−7,2	edge-P	148	eq	−78,7	face-P	106	ax	−16,8	edge-P	−126	eq	85,0	face-M
POGNII	δ	III	35	−32	−84	ax	−82,0	face-P	153	eq	36,6	edge-M	82	ax	13,1	edge-M	−161	eq	−83,6	face-P
	δ	III	36	−31	−81	ax	−75,8	face-P	154	eq	40,9	edge-M	82	ax	4,4	edge-M	−159	eq	−79,9	face-P
PPERHC	δ	II	26	0	−88	ax	−16,2	edge-P	142	eq	−56,4	face-P	114	ax	−18,5	edge-P	−116	eq	85,9	face-M
RHEPPO10	δ	III	27	−6	−90	ax	−59,1	face-P	150	eq	40,3	edge-M	105	ax	−38,1	edge-P	−127	eq	−76,7	face-P
SOZTEG	δ	III	17	−2	−102	ax	2,5	edge-M	136	eq	71,7	face-	114	ax	−19,0	edge-P	−124	eq	−89,8	face-P
SUKSIA	δ	III	46	−25	−68	ax	−39,6	edge-P	165	eq	−74,8	face-P	98	ax	−82,9	face-P	−140	eq	−6,1	edge-P
VIMGIH	δ	III	25	−3	−92	ax	26,5	edge-M	144	eq	70,4	face-M	122	eq	3,3	edge-M	−118	ax	−86,8	face-P
VIRFEH	δ	I	18	9	−97	ax	4,3	edge-M	137	eq	79,0	face-M	129	eq	−61,9	face-P	−106	ax	−59,0	face-P
WEHHIA	δ	III	25	−1	−90	ax	−53,9	face-P	141	eq	−67,6	face-P	115	ax	−60,5	face-P	−118	eq	−26,7	edge-P
YEPSAN	δ	III	36	−18	−79	ax	−39,7	edge-P	150	eq	−39,6	edge-P	96	ax	−20,2	edge-P	−134	eq	84,5	face-M
YEXZIK	δ	III	41	−28	−76	ax	−52,9	face-P	154	eq	−54,4	face-P	92	ax	56,7	face-M	−141	eq	51,9	face-M
YOYYUG	δ	III	33	−18	−83	ax	−66,4	face-P	149	eq	−45,8	face-P	97	ax	−10,1	edge-P	−137	eq	85,3	face-M
ZIPVAV	δ	III	45	−40	−74	ax	−74,6	face-P	160	eq	52,0	face-M	76	ax	5,3	edge-M	−161	eq	−84,0	face-P

[a] C_{ortho} of Ph4 is coordinated to the metal.

Table 11
Data of diphos complexes with a λ chelate ring (larger α angle at P1)

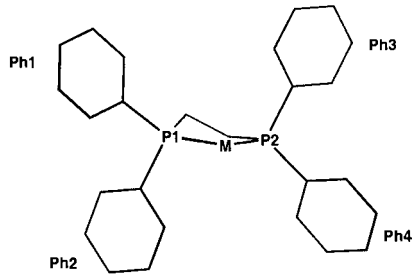

Complex	Ring	Conf.	P1	P2	Ph1				Ph2				Ph3				Ph4			
			α[°]	α[°]	β[°]	ax/eq	γ[°]	Orient.	β[°]	ax/eq	γ[°]	Orient.	β[°]	ax/eq	γ[°]	Orient.	β[°]	ax/eq	γ[°]	Orient.
BAYGEN	λ	II	−18	−4	−140	eq	74,5	face-M	92	ax	33,6	edge-M	123	ax	49,3	face-M	−133	eq	59,8	face-M
CASYAW	λ	II	−20	−1	−133	eq	67,9	face-M	97	ax	52,2	face-M	116	eq	−78,5	face−P	−112	ax	−14,8	edge-P
CULWIP	λ	II	−18	−5	−140	eq	−61,0	face-P	96	ax	−32,0	edge-P	115	ax	80,1	face-M	−123	eq	−8,6	edge-P
CUNMED	λ	III	−28	5	−153	eq	−63,4	face-P	83	ax	−20,4	edge-P	123	eq	−60,2	face-P	−113	ax	−62,3	face-P
DAJGEA	λ	III	−35	29	−154	eq	7,1	edge-M	81	ax	−2,7	edge-P	149	eq	28,8	edge-M	−92	ax	12,4	edge-M
DOBPOZ	λ	III	−26	2	−144	eq	−53,8	face-P	88	ax	−5,4	edge-P	123	eq	25,7	edge-M	−116	ax	69,2	face-M
DPERUB10	λ	III	−29	5	−150	eq	−43,2	edge-P	87	ax	7,8	edge-M	126	eq	75,9	face-M	−105	ax	11,4	edge-M
DUJXIP	λ	II	−17	−8	−136	eq	67,8	face-M	95	ax	−3,0	edge-P	103	ax	3,1	edge-M	−128	eq	69,7	face-M
	λ	I	−15	−12	−132	eq	69,6	face-M	99	ax	6,6	edge-M	99	ax	0,4	edge-M	−131	eq	68,3	face-M
DUMZIU	λ	II	−16	−7	−133	eq	45,8	face-M	103	ax	60,8	face-M	111	ax	79,0	face-M	−124	eq	−18,2	edge-P
GECLAB	λ	I	−15	−13	−128	eq	77,3	face-M	103	ax	36,5	edge-M	103	ax	32,7	edge-M	−131	eq	77,1	face-M
	λ	III	−26	4	−142	eq	63,6	face-M	94	ax	53,8	face-M	122	eq	12,6	edge-M	−115	ax	81,4	face-M

HACVOW01	λ	II	−22	−2	−143	eq	−58,7	face-P	95	ax	−13,0	edge-P	118	ax	14,4	edge-M	−120	eq	75,9	face-M
JIJFAJ	λ	I	−16	−8	−132	eq	−25,0	edge-P	102	ax	77,3	face-M	106	ax	−36,0	edge-P	−126	eq	−60,2	face-P
	λ	III	−24	1	−144	eq	−68,7	face-P	87	ax	−21,1	edge-P	118	ax	−3,8	edge-P	−119	eq	−60,1	face-P
KICZUR	λ	III	−31	10	−148	eq	41,2	edge-M	85	ax	56,5	face-M	127	eq	−88,6	face-P	−104	ax	35,8	edge-M
KOMPAD	λ	III	−31	13	−151	eq	−8,6	edge-P	87	ax	62,5	face-M	134	eq	9,7	edge-M	−103	ax	58,9	face-M
KURROE	λ	II	−25	0	−146	eq	89,6	face-M	89	ax	−3,7	edge-P	119	eq	38,6	edge-M	−117	ax	71,6	face-M
LEHZON	λ	I	−10	−9	−125	eq	57,3	face-M	110	ax	57,0	face-M	108	ax	−87,2	face-P	−130	eq	−28,0	edge-P
NABBEX	λ	III	−34	12	−150	eq	64,7	face-M	80	ax	20,1	edge-M	129	eq	−86,3	face-P	−102	ax	18,4	edge-M
PAFPAN	λ	II	−21	−8	−138	eq	61,9	face-M	91	ax	40,7	edge-M	110	ax	78,9	face-M	−124	eq	−17,6	edge-P
RERUHC10	λ	II	−16	−7	−133	eq	−61,5	face-P	102	ax	−44,8	edge-P	110	ax	67,6	face-M	−126	eq	41,4	edge-M
PIRKAC	λ	III	−30	9	−143	eq	73,8	face-M	82	ax	9,2	edge-M	123	eq	−85,2	face-P	−109	ax	19,8	edge-M
POGNEE	λ	III	−34	19	−149	eq	35,2	edge-M	83	ax	56,5	face-M	136	eq	−2,1	edge-P	−99	ax	81,7	face-M
PPERHC	λ	III	−32	11	−148	eq	68,5	face-M	85	ax	39,9	edge-M	129	eq	−70,8	face-P	−103	ax	7,5	edge-M
RHEPPO10	λ	III	−29	6	−151	eq	−76,1	face-P	84	ax	16,3	edge-M	130	eq	44,3	edge-M	−111	ax	63,1	face-M
VOLTIZ	λ	III	−30	6	−148	eq	−76,2	face-P	86	ax	−26,9	edge-P	126	eq	34,7	edge-M	−114	ax	−79,0	face-P
WEHHIA	λ	III	−33	11	−148	eq	74,7	face-M	77	ax	7,9	edge-M	126	eq	−77,7	face-P	−108	ax	−14,5	edge-P
WELVUE	λ	II	−20	0	−138	eq	5,1	edge-M	97	ax	62,7	face-M	122	eq	20,3	edge-M	−114	ax	64,3	face-M
WELWAL	λ	I	−13	−11	−127	eq	−19,1	edge-P	109	ax	42,9	edge-M	107	ax	62,8	face-M	−130	eq	−42,2	edge-P
WINJIM	λ	II	−19	−3	−144	eq	81,3	face-M	95	ax	36,8	edge-M	113	ax	78,8	face-M	−125	eq	20,1	edge-M
YEPSAN	λ	III	−27	5	−144	eq	29,8	edge-M	89	ax	62,8	face-M	123	eq	65,5	face-M	−109	ax	49,3	face-M
YETHUA	λ	I	−16	−13	−132	eq	75,6	face-M	99	ax	36,2	edge-M	102	ax	27,5	edge-M	−130	eq	73,8	face-M
	λ	I	−16	−14	−132	eq	73,0	face-M	97	ax	32,1	edge-M	101	ax	26,3	edge-M	−130	eq	76,2	face-M
YEXZEG	λ	III	−35	29	−151	eq	−33,6	edge-P	85	ax	65,3	face-M	159	eq	79,9	face-M	−83	ax	−4,5	edge-P
	λ	III	−37	33	−156	eq	−40,0	edge-P	81	ax	73,5	face-M	160	eq	82,7	face-M	−82	ax	−5,2	edge-P
YEXZIK	λ	II	−23	0	−140	eq	79,3	face-M	91	ax	4,4	edge-M	119	eq	83,5	face-M	−112	ax	30,8	edge-M
YIDTAG	λ	III	−26	3	−143	eq	−49,8	face-P	87	ax	−3,5	edge-P	122	eq	88,6	face-M	−116	ax	4,3	edge-M
YOYYUG	λ	III	−33	18	−149	eq	45,8	face-M	83	ax	66,4	face-M	137	eq	−85,3	face-P	−97	ax	10,2	edge-M
ZIPVEZ	λ	I	−14	−10	−128	eq	−45,5	face-P	107	ax	−51,7	face-P	105	ax	52,5	face-M	−132	eq	87,6	face-M

Table 12
Overview of phenyl ring chirality in diphos complexes with λ conformation

Chirality	Number of ligands
P^4	2
P^3M	3
P^2M^2	11
M^3P	14
M^4	10

envelope conformation there is a low edge–face selectivity of the phenyl rings bonded at P2 compared to the normal situation.

8. Comparison of the chiral diphenylphosphines

In the previous chapters, 40 complexes containing chiral bis(diphenylphosphanyl)ethane ligands were analyzed with regard to the chelate ring conformation and the orientation of the phenyl rings at the P atoms. As some compounds contain 2 phosphine ligands, the study includes a total of 50 ligands. The conformations of the chelate rings are divided into 3 groups (Fig. 3a–c): Half chair (type I), envelope (type II) and distorted envelope (type III). 20 chelate rings of type I, 13 chelate rings of type II and 17 of type III are found.

As already stated in the literature, the chirality of the chelate ring depends on the chirality of the ligand [7,8]. (*R*)- and (*R,R*)-phosphines form chelate rings with λ conformation, (*S*)- and (*S,S*)-ligands chelate rings with δ conformation, caused by the equatorial position of the substituents at the ethane bridge of the ligand. There are only 4 exceptions with the substituents in axial position.

The investigation of the arrangement of the phenyl rings reveils, that their orientation is not random, but controlled by the ligand chirality. Tables 7 and 8 summarize the correlation of the given ligand configuration and the chiral orientation of the phenyl rings of the PPh_2 groups.

In (*R*)-phosphine complexes phenyl ring orientations with P chirality preponderate, (*S*)-phosphines favor phenyl ring orientations with M chirality. For (*R*)-phosphine complexes P^4 and P^3M arrangements and for (*S*)-phosphine complexes M^4 and M^3P arrangements mean selectivity. In both cases M^2P^2 would indicate nonselectivity. For (*R*)-phosphine complexes PM^3 and M^4 and for (*S*)-phosphine complexes P^3M and P^4 would mean 'antiselectivity' contributing to an overall reduction of selectivity. However, no such 'antiselectivity' was found neither for (*R*)-phosphine nor for (*S*)-phosphine complexes. For a detailed sector analysis of the chiral bis(diphenylphosphanyl) ligands according to Fig. 5, see Section 10.

9. Diphos complexes as a reference group

To learn more on the mechanism of the chirality transfer, diphos (dppe) complexes which are chiral only because of their chelate ring conformations are included in the analysis as a reference group. To reduce the number of complexes, only the 52 compounds containing ruthenium and rhodium, found in the CSD, were taken into consideration (Table 9).

The diphos chelate rings were subdivided according to their chirality δ and λ. 40 ligands form λ chelate rings and 31 ligands form δ chelate rings. The data for the chelate conformations and the phenyl ring orientations are compiled in Tables 10 and 11.

The examination of the chelate ring conformations shows that type III chelate rings (distorted envelope) dominate. In the 40 λ cases 8 chelate rings are of type I (half chair), 12 of type II (envelope) and 20 of type III (distorted envelope). In the 31 crystal structures with δ chelate rings 4 have type I, 8 type II and 19 type III conformation. An extremely distorted envelope chelate ring is present in complex ZIPVAV with α values of 45° (P1) and −40° (P2).

The analysis of the chirality of the phenyl ring orientation leads to a surprising result (Tables 12 and 13). In crystal structures with λ chelate rings a preference of M chirality is observed. 10 ligands have M^4, 14 ligands M^3P and 11 ligands M^2P^2 chirality, whereas 3 ligands have P^3M and 2 ligands P^4 chirality. In complexes with δ chelate rings P chirality preponderates. 3 ligands have P^4, 11 ligands P^3M, 14 ligands M^2P^2 chirality, whereas 2 ligands have M^3P and 1 ligand has M^4 chirality. These results seem to be in contrast to the selectivity found in chiral bis(diphenylphosphanyl) ethane ligands, where λ chelate rings favor phenyl ring orientations with P chirality and vice versa.

The analysis of the population of the different sectors face-M, edge-M, edge-P and face-P by axial and equatorial phenyl rings, respectively, allows a more detailed examination of the selectivity. In complexes with envelope and distorted envelope chelate ring conformation only the 'steep' sides (P1) are taken into consideration, in half chair chelate ring complexes both sides are included. As most of the complexes have envelope or

Table 13
Overview of phenyl ring chirality in diphos complexes with δ conformation

Chirality	Number of ligands
P^4	3
P^3M	11
P^2M^2	14
M^3P	2
M^4	1

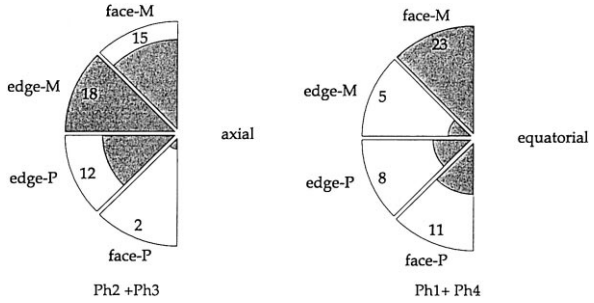

Fig. 6. Population of the different sectors according to Fig. 5 in λ chelate ring diphos complexes.

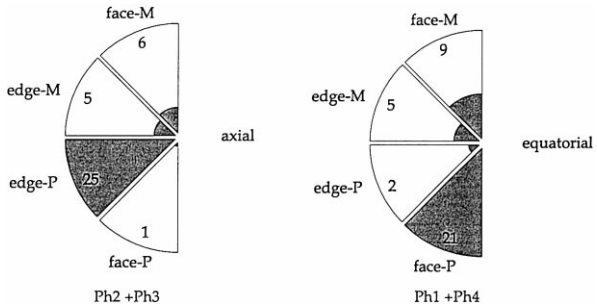

Fig. 8. Population of the different sectors according to Fig. 5 in complexes of (*R*)- and (*R,R*)-phosphine ligands.

distorted envelope chelate rings, this analysis deals mainly with phenyls at P1. The results are illustrated in Figs. 6 and 7.

In crystal structures with λ chelate rings equatorial phenyl rings are mainly in sector face-M (23), followed by sectors face-P (11) and edge-P (8). Axial phenyl rings do not favor a certain sector. They are distributed over the three sectors edge-M (18), face-M (15) and edge-P (12). The sector face-P seems to be 'forbidden'. Only 2 phenyl rings are found in this orientation. A comparable situation is encountered in the crystal structures with δ chelate ring conformations. The equatorial phenyl rings occupy mainly the sectors face-P (13) and face-M (12), followed by edge-M (7). The axial phenyl rings are found in three sectors, 15 in face-P, 11 in edge-M and 8 in edge-P. Sector face-M (1 ring) again seems to be 'forbidden'.

10. Discussion

The previous analysis showed, that in crystal structures with chiral bis(diphenylphosphanyl)ethane ligands there is selectivity in the phenyl ring orientations of the diphenylphosphanyl groups, depending on the chelate ring chirality and the axial or equatorial position, respectively. Phenyl rings in ligands with R chirality at the asymmetric center of the backbone and λ chelate ring conformation prefer P chirality, while those in ligands with S chirality and δ chelate ring conformation favor M chirality. In crystal structures with the achiral diphos ligand which adopts chiral chelate ring conformations the selectivity seems to be inverted. Here in complexes with λ chelate rings, the phenyl ring chirality M preponderates and vice versa. This, however, is a contradiction only at first sight because it disappears when a more detailed analysis of the population of the different sectors face-M, edge-M, edge-P and face-P (Fig. 5) as a function of the given chirality and the axial or equatorial character of the phenyl rings is carried out. This analysis is confined to both sides of chelate rings forming a half chair (type I) and to the 'steep' sides (P1) of envelope (type II) and distorted envelope chelate rings (type III), except for the second ligand of PNOBRH01, the 'steep side' of which is at P2. In addition, the 4 complexes with unusual chelate ring chirality are not taken into consideration. The sector analysis, which subdivides into that of axial phenyls and that of equatorial phenyls, is shown in Figs. 6–9 for the complexes of the chiral phosphines and diphos. It should be kept in mind that going from a λ to a δ chelate ring means an inversion at the line separating edge-M and edge-P.

The population analysis of axial phenyl rings in chiral phosphine complexes shows a clear dominance of only one sector (Figs. 8 and 9). In λ chelate ring complexes 25 out of 37 phenyls are found in sector edge-P, in δ chelate complexes 22 out of 30 phenyls are found in sector edge-M. Two other sectors are populated by a much lower number of phenyl rings, namely sectors edge-M and face-M for λ chelate rings

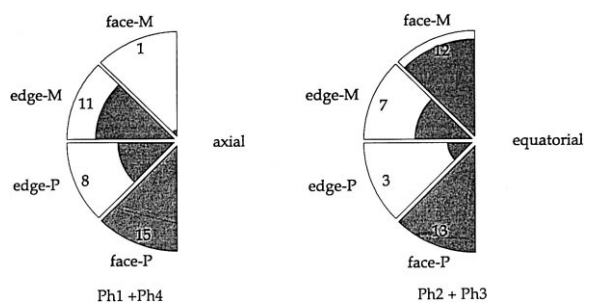

Fig. 7. Population of the different sectors according to Fig. 5 in δ chelate ring diphos complexes.

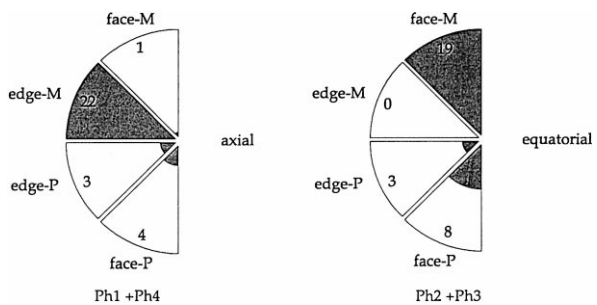

Fig. 9. Population of the different sectors according to Fig. 5 in complexes of (*S*)- and (*S,S*)-phosphine ligands.

(5 and 6, respectively) and sectors edge-P and face-P for δ chelate rings (3 and 4, respectively). One sector shows a conspicuously low population. It seems to be 'forbidden'. This sector is face-P for λ chelate rings and face-M for δ chelate rings. Both are occupied by only one ring.

In achiral diphos complexes, chiral only due to the chelate conformation, the selectivity is not as high as in the molecular structures of chiral phosphines. The axial phenyl rings are not only found in the sector preferred by the chiral phosphines, but also in the two sectors only partially occupied by the chiral phosphines. The axial phenyls are almost equally distributed over the sectors edge-P, edge-M, and face-M in λ chelate rings (12, 18, and 15 phenyl rings) and the sectors edge-M, edge-P, face-P in δ chelate rings (11, 8 and 15 phenyl rings). As for chiral phosphines the sector face-P in λ chelate rings and the sector face-M in δ chelate rings is 'forbidden' for diphos complexes.

In the case of the equatorial phenyl rings in chiral phosphines one sector dominates, face-P in λ chelate rings (21 of 37 cases) and face-M for δ chelate rings (19 of 30 cases). Also, the sectors face-M for λ chelate rings and face-P for δ chelate rings are populated to some extent. Independent of the chelate ring conformation the sectors edge-M and edge-P are little occupied.

By comparing the results of the chiral and achiral chelate phosphines conclusions to explain the selectivity can be drawn. In both chiral and achiral phosphines one sector, depending on the chirality of the chelate ring, is forbidden for axial phenyl rings. Obviously, this effect is independent of the additional substituents at the backbone in chiral phosphines. The steric effect causing the 'ban' of this sectors must be due to the chelate ring. A phenyl ring in the forbidden orientation (face-P in a λ chelate ring, face-M in a δ chelate ring) leads to an 1,3-interaction of CH_{ortho} with the axial CH of the chelate ring, resulting in steric hindrance.

The reason for the increased selectivity of the axial phenyls in chiral chelate phosphine complexes compared to the achiral diphos complexes is the substituent at the neighboring carbon atom of the chelate ring. Due to the interaction of CH_{ortho} with the equatorial substituent at this C atom the orientations edge-M and face-M are no longer favored in chiral λ chelate rings. The only sector, which is still 'allowed', is the sector edge-P, in which most of the axial phenyl rings are found (vice versa for δ chelate ring complexes).

In all the complexes of monosubstituted phosphines with the ring conformations envelope and distorted envelope the substituent is located at the C atom of the 'steep' side, called the P1-side in this analysis, except compound PNOBRH01, second ligand. The steric repulsion of the axial phenyl ring at P1 and the adjacent substituent at the ligand backbone may be one of the factors making the P1-side the 'steep' side of the chelate ring conformation. However, it should be kept in mind that in diphos complexes a lot of envelope and distorted envelope conformations are found, although there is no such substituent at the neighboring C atom (see above). It must be emphasized that in the present analysis only intra-chelate interactions have been taken into account. Crystal packing effects and interactions with the other ligands bound to the metal atoms, which cover an immense range, have not been considered.

Thus, the orientation of the axial phenyl rings in bis(diphenylphosphanyl)ethane complexes is dependent on two factors. The first is the 1,3-interaction between the axial phenyl rings and the axial C–H bonds in 3-position of the chelate ring. This effect can be observed in crystal structures of achiral as well as in chiral phosphines and leads to the 'ban' of one sector. The second factor is the steric repulsion of the axial phenyls and the neighbored substituents in chiral phosphines. This repulsion leads to the dominance of only a narrow sector for the phenyl orientation. It is very likely, that the axial phenyl rings influence the arrangement of the equatorial phenyls, thus, contributing to the chiral pocket formed by the four phenyl rings of bis(diphenylphosphanyl)ethane ligands.

11. Experimental part

A search in the Cambridge Structural Database (CSD) [97] for structures of the type $L_nM(Ph_2P\text{-}CHR\text{-}CHR'\text{-}PPh_2)_m$, (M = transition metal; $m = 1$ or 2) was carried out in November 1996. The atomic coordinates were extracted in SYBYL MOL2 format. The angles were obtained from the files using the program SYBYL [98]. All values have been compared with original values retrieved directly from the Database to exclude conversion mistakes. These efforts were necessary, because the original values could not be assigned unambiguously to certain phenyl rings. Some complexes crystallize in centrosymmetric space groups (CASDOP, FUTLUB, KIGTID, YIFCOF, FUTWUM, FUTXAT). In the compound VIMBEY the crystal contains 30% of the other diastereomer. In these cases only the enantiomer–diastereomer found in the database was included in the present analysis. In some structures there are more than one independent species in the unit cell, or the complex consists of two chelate rings with bisphosphines. In these cases all the independent species/chelate rings were subjected to the present analysis. Data of the unpublished crystal structures COCONO and FP14 were retrieved with help of the program PLATON [99]. The search in the CSD [97] for structures of the type $L_nM(diphos)_m$ (M = Ru, Rh; $m = 1$ or 2) was carried out in February 1997. In some of the complexes with the achiral ligand diphos the space groups are chiral (CULWOV, FUVPER, LEMLOE, SUKSIA). This ef-

fect is caused by either chiral coligands (CULWOV, LEMLOE) or by self-resolution (FUVPER, SUKSIA).

Acknowledgements

We thank the Fonds der Chemischen Industrie for support of this work.

References

[1] H. Brunner, M. Janura, Synthesis, in press.
[2] I. Ojima, Catalytic Asymmetric Synthesis, VCH, New York (1993).
[3] K.E. Koenig, In: J.D. Morrison (Ed.), Asymmetric Synthesis, Vol. 5, Academic Press, Orlando (1993) p. 71.
[4] H. Brunner, M. Muschiol, F. Prester, Angew. Chem., Int. Ed. Engl. 29 (1990) 653. Angew. Chem., Int. Ed. Engl. 29 (1990) 653.
[5] M. Lautens, J.C. Lautens, A.C. Smith, J. Am. Chem. Soc. 112 (1990) 5627.
[6] W.S. Knowles, B.D. Vineyard, M.J. Sabacky, B.R. Stults, Fundam. Res. Homogeneous Catal. 3 (1978) 537.
[7] D. Seebach, E. Devaquet, A. Ernst, M. Hayakawa, F.N.M. Kühnle, W.B. Schweizer, B. Weber, Helv. Chim. Acta 78 (1995) 1636.
[8] F. Basolo, R.G. Pearson, Mechanisms of Inorganic Reactions, Wiley, New York (1976) p. 336.
[9] Inorg. Chem., 9 (1970) p. 1.
[10] The compounds COCONO, DIRE and FP14 were taken from the original literature. Their names are not CSD codes.
[11] F. Morandini, G. Consiglio, B. Straub, G.F. Ciani, A. Sironi, J. Chem. Soc., Dalton. Trans. (1983) 2293.
[12] G. Consiglio, F. Morandini, G.F. Ciani, A. Sironi, M. Kretschmer, J. Am. Chem. Soc. 105 (1983) 1391.
[13] A. Dietl, PhD Thesis, University of Regensburg (1994).
[14] G. Consiglio, F. Morandini, G.F. Ciani, A. Sironi, Organometallics 5 (1986) 1976.
[15] R.H. Morris, J.F. Sawyer, A. Sella, Acta Crystallogr., C (Cr. Str. Comm.) 44 (1988) 23.
[16] F. Morandini, G. Consiglio, A. Sironi, Gazz. Chim. Ital. 117 (1987) 61.
[17] F. Morandini, G. Pilloni, G. Consiglio, A. Sironi, M. Moret, Organometallics 12 (1993) 3495.
[18] M.C.B. Colbert, A.J. Edwards, J. Lewis, N.J. Long, N.A. Page, D.G. Parker, P.R. Raithby, J. Chem. Soc, Dalton Trans. (1994) 2589.
[19] D.H. Farrar, N.C. Payne, J. Am. Chem. Soc. 107 (1985) 2054.
[20] I.S. Thorburn, S.J. Rettig, B.R. James, Inorg. Chem. 25 (1986) 234.
[21] C.G. Young, S.J. Rettig, B.R. James, Can. J. Chem. 64 (1986) 51.
[22] R.G. Ball, N.C. Payne, Inorg. Chem. 16 (1977) 1187.
[23] L.J. Farrugia, N. McDonald, R.D. Peacock, J. Cluster Sci. 5 (1994) 341.
[24] J.M. Brown, P.L. Evans, P.J. Maddox, K.H. Sutton, J. Organomet. Chem. 359 (1989) 115.
[25] F. Morandini, G. Consiglio, A. Sironi, M. Moret, J. Organomet. Chem. 370 (1989) 305.
[26] E.P. Kyba, R.E. Davis, P.N. Juri, K.R. Shirley, Inorg. Chem. 20 (1981) 3616.
[27] H. Brunner, A.F.M.M. Rahman, I. Bernal, Inorg. Chim. Acta 83 (1984) L93.
[28] W.J. Halg, L.R. Ohrstrom, H. Ruegger, L.M. Venanzi, T. Gerfin, V. Gramlich, Helv. Chim. Acta 76 (1993) 788.
[29] H. Nishiyama, H. Brunner, P.G. Jones, J. Organomet. Chem. 405 (1991) 247.
[30] R.E. Davis, B.B. Meyer, K.L. Hassett, P.N. Juri, E.P. Kyba, Acta Crystallogr., C (Cr. Str. Comm.) 40 (1984) 21.
[31] H. Brunner, G. Vitulli, W. Porzio, M. Zocchi, Inorg. Chim. Acta 96 (1985) 67.
[32] D.L. Allen, V.C. Gibson, M.L.H. Green, J.F. Skinner, J. Bashkin, P.D. Grebenik, J. Chem. Soc., Chem. Comm. (1983) 895.
[33] D. Fenske, A. Christidis, Z. Naturforsch. B 38 (1983) 1295.
[34] T. Minami, Y. Okada, R. Nomura, S. Hirota, Y. Nagahara, K. Fukuyama, Chem. Lett. (1986) 613.
[35] F.A. Cotton, S.J. Kang, Inorg. Chim. Acta 209 (1993) 23.
[36] U. Nagel, B. Rieger, Chem. Ber. 121 (1988) 1123.
[37] F.A. Cotton, E.C. DeCanio, P.A. Kibala, K. Vidyasagar, Inorg. Chim. Acta 184 (1991) 221.
[38] K. Saito, S. Saijo, K. Kotera, T. Date, Chem. Pharm. Bull. 33 (1985) 1342.
[39] H. Brunner, P. Faustmann, publication in preparation.
[40] M.I. Bruce, M.P. Cifuentes, M.G. Humphrey, E. Poczman, M.R. Snow, E.R.T. Tiekink, J. Organomet. Chem. 338 (1988) 237.
[41] J.L. Bookham, W. McFarlane, M. Thornton-Pett, S. Jones, J. Chem. Soc., Dalton Trans. (1990) 3621.
[42] R.D. Adams, A. Davidson, J.P. Selegue, J. Am. Chem. Soc. 101 (1979) 7232.
[43] J.D. Oliver, D.P. Riley, Organometallics 2 (1983) 1032.
[44] A. Saare, L. Dahlenburg, Z. Naturforsch. B 47 (1992) 247.
[45] Chung-Yuan Liu, Ming-Chu Cheng, Shie-Ming Peng, Shiuh-Tzung Liu, Organometallics, 13 91994) 4294.
[46] H. Brunner, B. Hammer, C. Krüger, K. Angermund, I. Bernal, Organometallics 4 (1985) 1063.
[47] D.A. Slack, I. Greveling, M.C. Baird, Inorg. Chem. 18 (1979) 3125.
[48] H.B. Kagan, Comprehensive Organometallic Chemistry, Vol. 8, In: G. Wilkinson, F.G.A. Stone, E.W. Abel (Eds.), Pergamon, Oxford (1982) p. 463.
[49] H. Brunner, Angew. Chem. 95 (1983) 921. Angew Chem. Int. Ed. Engl. 22 (1983) 897.
[50] R.O. Gould, T.A. Stephenson, M.A. Thomson, J. Chem. Soc., Dalton Trans. (1981) 2508.
[51] W.C. Fultz, A.L. Rheingold, P.E. Kreter, D.W. Meek, Inorg. Chem. 22 (1983) 860.
[52] G. Smith, D.J. Cole-Hamilton, M. Thornton-Pett, M.B. Hursthouse, J. Chem. Soc., Dalton Trans. (1983) 2501.
[53] R.G. Ball, F. Edelmann, G.-Y. Kiel, J. Takats, R. Drews, Organometallics 5 (1986) 829.
[54] H. Lehner, D. Matt, A. Togni, R. Thouvenot, L.M. Venanzi, A. Albinati, Inorg. Chem. 23 (1984) 4254.
[55] M.I. Bruce, T.W. Hambley, M.R. Snow, A.G. Swincer, Organometallics 4 (1985) 501.
[56] G.J. Baird, S.G. Davies, S.D. Moon, S.J. Simpson, R.H. Jones, J. Chem. Soc., Dalton Trans. (1985) 1479.
[57] M.I. Bruce, C. Dean, D.N. Duffy, M.G. Humphrey, G.A. Koutsantonis, J. Organomet. Chem. 295 (1985) C40.
[58] C.G. Pierpont, R. Eisenberg, Inorg. Chem. 12 (1973) 199.
[59] R.R. Burch, J.C. Calabrese, J. Am. Chem. Soc. 108 (1986) 5359.
[60] J. Pursiainen, T.A. Pakkanen, J. Organomet. Chem. 309 (1986) 187.
[61] M.I. Bruce, P.A. Humphrey, M.R. Snow, E.R.T. Tiekink, J. Organomet. Chem. 303 (1986) 417.
[62] M.I. Bruce, M.G. Humphrey, M.R. Snow, E.R.T. Tiekink, J. Organomet. Chem. 314 (1986) 213.
[63] M.I. Bruce, A. Catlow, M.G. Humphrey, G.A. Koutsantonis,

M.R. Snow, E.R.T. Tiekink, J. Organomet. Chem. 338 (1988) 59.
[64] S.J. Sherlock, M. Cowie, E. Singleton, M.M. de V. Steyn, Organometallics 7 (1988) 1663.
[65] S. Suravajjala, L.C. Porter, Acta Crystallogr. C (Cr. Str. Comm.) 49 (1993) 1456.
[66] W.H. Pearson, J.E. Shade, J.E. Brown, T.E. Bitterwolf, Acta Crystallogr. C (Cr. Str. Comm.) 52 (1996) 1106.
[67] S. Chang-Ping, W. Je-Yu, G. He-Fu, X. Wen-Qing, L. Xiu-Yun, W. Jia-Huai, Jiegou Huaxue (J. Struct. Chem.) 9 (1990) 301.
[68] T.S. Lobana, R. Singh, E.R.T. Tiekink, J. Coord. Chem. 21 (1990) 225.
[69] M.A. Massa, T.B. Rauchfuss, S.R. Wilson, Inorg. Chem. 30 (1991) 4667.
[70] R.D. Adams, Z. Li, J.-C. Lii, W. Wu, J. Am. Chem. Soc. 144 (1992) 4918.
[71] N.G. Connelly, P.M. Hopkins, A.G. Orpen, G.M. Rosair, F. Viguri, J. Chem. Soc., Dalton Trans. (1992) 2907.
[72] D. Carmona, M.P. Lamata, J. Ferrer, J. Modrego, M. Perales, F.J. Lahoz, R. Atencio, L.A. Oro, J. Chem. Soc., Chem. Comm. (1994) 575.
[73] D.D. Pathak, H. Adams, C. White, J. Chem. Soc., Chem. Comm. (1994) 733.
[74] J. Lewis, N.A. Page, P.R. Raithby, M. Younus, Private communication, 1995.
[75] W.A. Schenk, T. Stur, E. Dombrowski, Inorg. Chem. 31 (1992) 723.
[76] G. Bruno, G. De Munno, G. Tresoldi, S. Lo Schiavo, P. Piraino, Inorg. Chem. 31 (1992) 1538.
[77] M.R. Churchill, R.A. Lashewycz, Inorg. Chem. 17 (1978) 1950.
[78] P. Albano, M. Aresta, M. Manassero, Inorg. Chem. 19 (1980) 1069.
[79] D. Touchard, C. Morice, V. Cadiero, P. Haquette, L. Toupet, P.H. Dixneuf, J. Chem. Soc., Chem. Comm. (1994) 859.
[80] J.R. Polam, L.C. Porter, J. Coord. Chem. 29 (1993) 109.
[81] M.C. Hall, B.T. Kilbourn, K.A. Taylor, J. Chem. Soc., A (1970) 2539.
[82] J.A. McGinnety, N.C. Payne, J.A. Ibers, J. Am. Chem. Soc. 91 (1969) 6301.
[83] A.G. Becalski, W.R. Cullen, M.D. Fryzuk, B.R. James, G.-J. Kang, S.J. Rettig, Inorg. Chem. 30 (1991) 5002.
[84] K. Kirchner, K. Mauthner, K. Mereiter, R. Schmid, J. Chem. Soc., Chem. Comm. (1993) 892.
[85] E.R.T. Tiekink, T.S. Lobana, R. Singh, J. Cryst. Spectro. 21 (1991) 205.
[86] J.D. Gargulak, M.D. Noirot, W.L. Gladfelter, J. Am. Chem. Soc. 113 (1991) 1054.
[87] G.E. Ball, W.R. Cullen, M.D. Fryzuk, B.R. James, S.J. Rettig, Organometallics 10 (1991) 3767.
[88] Z. Atherton, C.W. Faulkner, S.L. Ingham, A.K. Kakkar, M.S. Khan, J. Lewis, N.J. Long, P.R. Raithby, J. Organomet. Chem. 462 (1993) 265.
[89] J.D. Gargulak, W.L. Gladfelter, Inorg. Chem. 33 (1994) 253.
[90] K.J. Adams, T.D. McGrath, A.J. Welch, Acta Crystallogr. C (Cr. Str. Comm.) 51 (1995) 401.
[91] C.W. Faulker, S.L. Ingham, M.S. Khan, J. Lewis, N.J. Long, P.R. Raithby, J. Organomet. Chem. 482 (1994) 139.
[92] D. Touchard, P. Haquette, A. Daridor, L. Toupet, P.H. Dixneuf, J. Am. Chem. Soc. 116 (1994) 11157.
[93] B. Chin, A.J. Lough, R.H. Morris, C.T. Schweitzer, C. D'Agostino, Inorg. Chem. 33 (1994) 6278.
[94] S.J. Skoog, J.P. Campbell, W.L. Gladfelter, Organometallics 13 (1994) 4137.
[95] B.T. Heaton, C. Jacob, A.K. Smith, M. Quayle, Rhodium Express 1 (1993) 18.
[96] K. Mauthner, K. Mereiter, R. Schmid, K. Kirchner, Inorg. Chim. Acta 236 (1995) 95.
[97] F.H. Allen, O. Kennard, Chemical Design Automatation News 8 (1) (1993) 31.
[98] Sybyl Version b.1, Tripos, Inc.
[99] A.L. Spek, Platon 92, graphic program, University of Utrecht, Netherlands (1992).